International Journal of Research Publication and Reviews

Journal homepage: www.ijrpr.com ISSN 2582-7421

A Review for the Formability of Single-Point Incremental Forming (SPIF) Process

"Lecturer Dr. Aws Khalid Ibrahim"

"Al-Karkh University of Science, College of Remote Sensing and Geophysics, Baghdad, Iraq"

DOI: https://doi.org/10.55248/gengpi.2022.3.8.36

A B S T R A C T

Traditional manufacturing operations require a long time and capital for prototype development and small batch production. Forming processes necessitate component specific and expensive dies since their preparation and design are time-consuming. In latest years, incremental sheet metal forming has acquired good attraction owing to its ability for small-batch productions and prototyping with generic tooling and short lead time. In this paper, a review of literature works has been presented describing investigations carried out on the formability of lightweight alloys, mainly Al alloys, Ti alloys and Mg alloys, during single point incremental forming (SPIF) process, considering the deformation mechanism, formability assessment techniques, forming limit curves, effects of influencing factors, and the effect of heating.

Keywords: Single point incremental forming (SPIF), formability, deformation, forming limit diagram (FLD), forming limit curve (FLC).

1. Introduction

Ideas necessitate be converting quickly into products and analyzing to fulfill the prerequisites of the industrial revolution. Manufacturing operations having less tooling cost and changeover time can meet the requirement of prototype development and mass customization. The prototype permits the enhancement of the design in the crucial stages of product development. Traditional manufacturing operations necessitate a long time and capital for prototype development and small batch production. Forming processes necessitate component specific and expensive dies since their preparation and design are time-consuming. In latest years, incremental sheet metal forming has acquired good attraction owing to its ability for small-batch productions and prototyping with generic tooling and short lead time [1].

In Incremental Sheet Forming (ISF), as the substitute to the traditional technique, the rotating mandrel tool progressively sinks into the sheet, therefore leading to an increasing degree of the material deformation. This type of ISF is called Single-Point Incremental Forming (SPIF). Whilst in Two-Point Incremental Forming (TPIF), a counter tool is adopted that travels on the opposite surface of the sheet (Figure 1) [2].

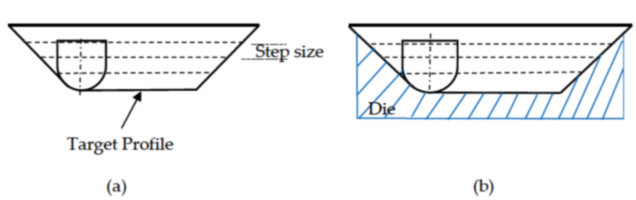

Fig. 1- Schematics of ISF Processes (**a**) SPIF; (**b**) TPIF.

2. Formability of SPIF

This section illustrates investigations performed on the formability of lightweight metals and alloys, primarily Al alloys, Ti alloys and Mg alloys, throughout SPIF, considering the deformation mechanism, formability assessment techniques, forming limit curves, effects of influencing factors, and the effect of heating.

2.1. Deformation Mechanism

Madeira et al. [3] concluded that failure and plastic flow in SPIF ocuur by the crack opening mode under tensile stresses. Li et al. [4] explored strain evolutions and deformation modes during the SPIF of 7075-O aluminium alloy sheet throughout finite element simulations utilizing solid elements. Simulation results indicated that a combination of shearing, bending, and stretching has taken place in incrementally formed cone shape, and the major deformation mode was found to be a strain component perpendicular to the tool direction. Ai et al. [5] established an analytical model to investigate the deformation behavior of two aluminium alloys: AA5052 and AA1100, through SPIF. It has been concluded that the deformation was appreciably affected by bending, and the commencement of fracture has been seen to be dependent on both sheet material ductility and stability of deformation. By means of finite element simulations and experimental investigations, Said et al. [6] has shown that a combination of higher values of sheet thickness and forming wall angle accompanied with small radius of forming tool could increase the damage of the AA1050 sheet in SPIF. Maqbool and Bambach [7] explored the contributions of various deformation modes of, i.e., the shearing, bending, and stretching of an Al sheet in SPIF, utilizing finite element simulations, incremental sheet-forming experiments, and analytical modeling. Sensitivity to the deformation modes has been deliberated by considering the process variables namely, tool step-size, tool radius, friction, wall angle, and sheet thickness. The bending deformation mode was shown to be more outstanding for larger tool radii, and shear deformation was seen to be considerable for larger sheet thickness. Esmaeilpour et al. [8] proved that the yield criterion Yld2004-18p was more precise for the representation of the deformation of an AA2024 sheet during SPIF.

Esmaeilpour et al. [9] has carried out finite element simulations of SPIF of a 7075-O alloy sheet using 3D yield function specified throughout the crystal plasticity material model and 3D representative elementary volume (RVE) technique. The results of finite element simulation of effective strain, tool force, and thickness distributions adopting two yield criteria, i.e., Yld2004-18p and Hill 1948 have been compared. Mirnia et al. [10] explored the evolution of damage in two-stage SPIF of AA6061-T6 sheet utilizing the finite element analysis and the three-parameter Modified Mohr–Coulomb (MMC3) fracture criterion. It was shown that the strategy of two-stage forming could form a sound part with lesser damages than that achieved by solo-stage SPIF. Ilyas et al. [11] explored the mechanics of SPIF deformation of AA2024-O sheet based on the finite element simulation and Gurson–Tvergaard–Needleman damage model of a straight groove test adopting solid elements. Failure has been found to take place in the sheet in SPIF when the value of damage parameter approaches to 1, regardless of the forming conditions. Modes of deformation in SPIF include shearing, bending, and stretching owing to the cyclic nature of the loading as a result of the overlapping toolpath. A couple of failure types, namely fracture-initiated and necking-initiated, have been observed through SPIF, and localized deformation throughout thickness shear led to greater formability of SPIF [12]. Shrivastava and Tandon [13] presented that the AA1050 sheet formability in SPIF has been improved owing to a change of texture from cube type to brass and P-type. Mishra et al. [14] demonstrated that plain strain with through-thickness shear TTS existed in the wall region of incrementally formed parts and (TTS) considerably affected deformation through SPIF. Sheet anisotropy in yield strength through the incremental forming was owing to the existence of a brass component established by the average Schimd factor. Hussain et al. [15] stated that micro-structural changes of aluminium alloys in SPIF, i.e., AA6061 and AA5754, resulted in reduction in ductility with improvement in strength. Kumar and Maji [16] demonstrated that the deformation mechanism due to instability determined the limit strains and restricted the forming limit angle in SPIF of truncated drawpieces (Figure 2).

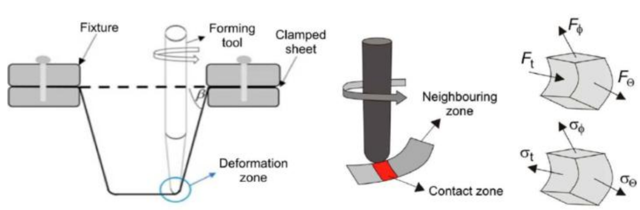

Fig.2- The deformation region in SPIF with the state of stress and forces acting [16].

2.2. Forming Limit Curves

Madeira et al. [3] estimated the FLC based on strain pairs in fracture of truncated cone shapes of an AA1050-H111 sheet via SPIF. It was found that when employing a gauge length, fracture strain could avert the scattering of measured limit strain pairs obtained experimentally and the dependence of the part geometry and forming tool in predicting FLC. Lu et al. [17] detected that throughout the double-sided incremental forming, the fracture forming limit could be increased compared to that of SPIF by applying various magnitudes of tool shift and supporting force. Do et al. [18] showed that the formability of an formed aluminium sheet was higher than that of the flat one in terms of highest formable wall angle during SPIF of a cone shaped component via a CNC machine. Do et al. [19] estimated a forming limit curve based on fracture strains for equi-biaxial strain and plane strain deformations produced via incremental sheet-forming tests. Results of finite element simulation of plastic strains were seen to be in good match with the experimental values for an AA5052-O sheet. Mirnia and Shamsari [20] predicted ductile fracture in SPIF of an AA6061-T6 aluminium alloy sheet in finite element simulation using a modified Mohr–Coulomb model. It was shown from the fracture strains via numerical predictions that the limit diagram of fracture-forming under non-proportional loading was dissimilar in magnitude and shape from that attained for proportional loading. Gatea et al. [21] performed finite element investigation to estimate the fracture during SPIF of pure titanium sheet utilizing various damage models based on deformation modes and stress triaxiality. It was found that the forming limit curve at fracture zone for titanium sheet by SPIF estimated by numerical simulations was in good match with that attained by the Nakazima test. Yoganjaneyulu et al. [22] determined that higher speed and larger tool size resulted in better formability during SPIF of a titanium Grade 2 sheet. Wang et al. [23] presented that the formability of AA2024 sheets with various conditions of heat treatment was enhanced at high temperature with a low pitch and higher feed rate. Zhan et al. [24] also demonstrated a higher formability of an AA2024-T3 sheet at higher tool rotational speed compared with that of conventional SPIF. Yoganjaneyulu et al. [25] presented that the forming limit of the topmost sheet was maximum in the case of multi-sheet incremental forming of a titanium sheet, and it decreased towards the bottom sheets. Kumar and Maji [26] presented the estimations of the forming limit of aluminium alloy sheets during SPIF via the deformation instability method (Figure 3).

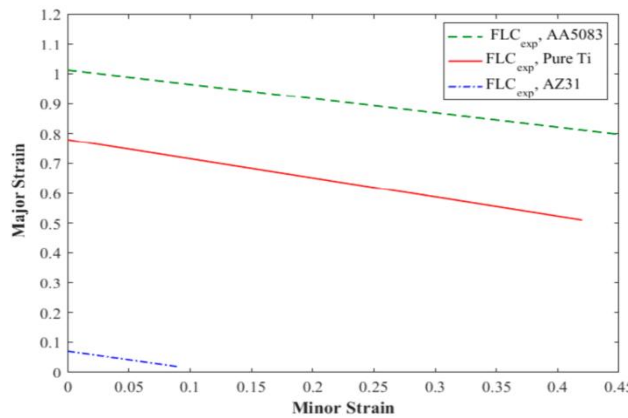

Fig.3- The incremental sheet-forming process showing plots of FLCs [26].

2.3. Effects of Process Parameters on Formability

Jeswiet et al. [27] investigated the design process of SPIF, in view of production time, surface roughness, and formability by using various geometries of the forming tool. It has been found that a flat-ended tool offered the best combination of low surface roughness and good formability. Azevedo et al. [28] explored the influences of diverse types of lubricants such as AL-M, SAE30, AS-40, and B5746 on the AA1050 parts formed via SPIF. It has been noticed that the surface finish of the formed component depends on the type of lubricant. Behera et al. [29] dealt with dimensional accuracy when shaping a clinical implant of titanium sheet through SPIF process utilizing free form surface model and the multivariate adaptive regression spline function. The proposed approach demonstrated higher dimensional accuracy and better shape of the titanium implant fabricated via SPIF. Lu et al. [30] performed investigational studies on incremental forming of a customized cranial plate made from a pure titanium sheet. The thickness distributions and surface finish of the formed plate were observed to be relevant to cranioplasty. Bastos et al. [31] recommended an appropriate parameters and process setup to develop the efficiency of forming time in SPIF.

Vanhove et al. [32] proved that the thin-shelled clavicle implants of titanium could be formed via SPIF with acceptable accuracy. Formisano et al. [33] noticed a better formability achieved by positive incremental forming than the negative method. Uheida et al. [34] explored the influences of directions of tool rotation on the formability of a titanium sheet during SPIF process. The toolpath climb strategy has been presented to give better formability in terms of a greatest forming wall angle and superior accuracy. Khan et al. [35] studied the influences of various heat treatments on the formability of Al-2219 sheet through SPIF operation. Minimum form error and high formability were realized via the solution with treatment incremental forming age hardening route. Tera et al. [36] proposed strategies of two-stage forming consisting of finishing and roughening as the most appropriate avenues based upon analytic hierarchy order. Palumbo et al. [37] accomplished enhanced formability of biocompatible AZ31B magnesium alloy sheet at high rotational speed of the forming tool with delayed cytotoxic influence.

Kumar et al. [38] presented a parametric study on formability of AA2024-O sheet through SPIF process. The researchers found that the formability was most appreciably influenced by the step size and wall angle. Kumar and Gulati [39] carried out ivestigations on the influences of process parameters on surface finish of the resulted surface during the incremental forming of aluminium alloy sheets based upon Taguchi method and Design of Experiments. Tool diameter has been noticed as the most effective factor influencing surface quality along with lubricant viscosity and tool shape. An optimal set of input parameters has been specified to reach a better surface quality. Oraon and Sharma [40] constructed an artificial neural network model to estimate surface roughness through SPIF of an AA3003-O alloy sheet adopting six input process parameters such as feed rate, step depth, spindle speed, lubricant density, wall angle, and sheet thickness. The model developed has been observed to predict surface roughness in the incremental forming operation with acceptable dimensional accuracy. Su et al. [41] explored the influences of relevant process parameters on the formability of an AZ31 magnesium alloy sheet through SPIF, and they recommended forming tool radius of 5 mm, a forming temperature of 250 ^{o}C, and a feed rate of 0.7 mm as the most significant factors. De Castro Maciel et al. [42] showed that adhesion on the tool influences the material deformation of magnesium and aluminium alloys during SPIF process when adopting a forming tool with roller ball. Maji and Kumar [43] performed multi-objective optimization of the formability of an AA5083 sheet through SPIF considering the deformed sheet thickness, surface roughness, and forming wall angle as measures of formability.

Murugesan and Jung [44] inspected the formability of an AA3003-H18 sheet during SPIF process utilizing response surface methodology and Design of Experiments to identify the optimal parameters of forming. Gatea and Ou [45] carried out investigational experiments on various values of surface roughness in incrementally formed sheets of grade 1 pure titanium taking into consideration the process parameters such as feed rate, step size, and tool diameter. It was noticed that surface roughness differed with the deformation depth of the incrementally formed part, and a rough surface could be realized in zones with low equivalent plastic strain and high equivalent stress.

2.4. Heat-Assisted Formability

Incremental forming of higher harness materials as well as materials with lower ductility such as Mg-alloy and titanium sheets has been made possible by applying heat utilizing different methods [46], and heat-assisted formability was observed to be larger than that at room temperature. There are two commonly adopted methods of heating the workpiece during SPIF: air assisted (Figure 4a) and tool assisted (Figure 4b).

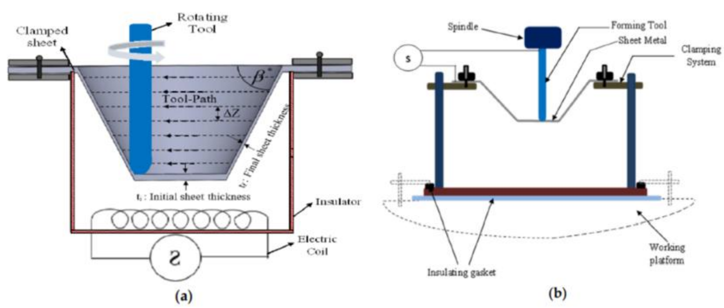

Fig.4- Incremental sheet forming with (a) air-assisted heating; (b) tool-assisted heating [46].

2.4.1. Tool Assisted Heating

Ambrogio and Gagliardi [47] performed investigational studies on the formability and temperature distributions during high-speed SPIF process of two lightweight alloys, i.e., Ti6-Al-4V, and AA5754 adopting coil pitch and tool velocity. It has bee concluded that the optimal set of process parameters for a sheet material could not only improve part quality and productivity but also enhance formability at high working temperatures. Khazaali and Saniee [48] explored the influences of the input process parameters, namely sheet temperature, , tool diameter and vertical pitch on thickness reduction and formability through warm incremental forming of Ti-6Al-4V sheet. Drawing depth and formability before fracture have been observed to be larger for higher values of tool diameter and vertical pitch. The temperature of sheet material was considerably affected by input factors and interfacial friction. Springback and flow stress have been reduced at elevated working temperatures.

Explorations have been performed on electric hot incremental forming of Ti alloy sheets as well as the formability at high temperatures with appropriate process parameters has been discussed [49]. Bao et al. [50] proved an important enhancement in the formability of AZ31B magnesium alloy during SPIF process owing to sheet heating by applying electric pulsed current between the sheet material and the forming tool. Husmann and Magnus [51] proposed an approach of measuring temperature of the workpiece through the incremental sheet forming by thermography. Gupta and Jeswiet [52, 53] found that frictional heating of an AA5754-H32 sheet in SPIF process was appreciably affected by the lubrication conditions at the tool–sheet interface and the geometry to be formed. Pacheco and Silveira [54] realized a reduction in forming forces through electric hot incremental forming of an AA1050 sheet accompanied with preheating compared to that without preheating. Grimm and Ragai [55] attained a better surface finish and enhanced formability in electrically-assisted forming of Ti sheet by applying liquid metal lubrication.

Riaz et al. [56] noticed that an increase in the rotational speed of the forming tool has increased the temperature and accordingly influenced the microstructures in incremental forming of aerospace alloy.

2.4.2. Air-Assisted Heating

The Taguchi approach was applied to determine the optimal processing conditions and to carry out a parametric study in warm incremental forming of titanium alloy by Khazaali and Saniee [57, 58] throughout a simple groove test, and this was verified by experimental tests. Leonhardt et al. [59] presented the accomplishment of a constant homogeneous temperature during SPIF of an AZ31 magnesium alloy sheet via the hot air heating approach. The forming force was reduced at an elevated temperature and the highest forming angle of 50^{o} was attained at a temperature of 300 ^{o}C with an orange peel effect. Liao et al. [60] determined better surface quality of AZ31B magnesium alloy sheet during incremental forming by adopting hot air heating compared that produced by far-infrared heating, and the distributions of temperature largely affected by the orange peel effect. Mugendiran and Gnanavelbabu [61] proved that measurements of strain during SPIF of an AA5052 sheet utilizing the digital image processing approach could reduce errors in measurement for predicting the forming limit diagram. Lee and Yang [62] accomplished a considerable enhancement of formability of an AZ31 magnesium alloy sheet in terms of the angle representing the forming limit during incremental forming by using a near-infrared heater. Throughout the experimental study on various tool lubricants and materials, Singh et al. [63] showed that molybdenum disulphide and tool steel (EN-31) a mixture were appropriate for hot incremental forming of aluminium alloy sheets.

3. Conclusion

This work presents a review of aspects of in-progress research on SPIF of light-weight materials. The following remarks about SPIF formability can be summarized as:

1- Owing to its good formability, aluminium is the dominant material under investigation in SPIF.

2- Among the sheet materials mentioned in the literature, the least investigated metals are titanium and its alloys and magnesium alloys.

3- Improvement of the formability of these materials was accomplished via using processes performed at elevated temperatures.

4- Due to the relations between process parameters and their various influences when forming diverse materials, there are many conflicts in the effect of process parameters on the sheet formability. Moreover, only two fundamental shapes of test objects are adopted: truncated pyramids and truncated cones.

5- Various shapes of the final component and the variety of lubricants used make it difficult to make a good comparison among data for different materials.

.

References

[1] Sattar Ullah, Peng Xu, Xiaoqiang Li, Yanle Li, Kai Han and Dongsheng Li. A Review on Part Geometric Precision Improvement Strategies in Double-Sided Incremental Forming. Metals 2022, 12, 103.
[2] Tomasz Trzepieci´nski, Sherwan Mohammed Najm, Valentin Oleksik, Delia Vasilca, Imre Paniti and Marcin Szpunar
[3] Madeira, T.; Silva, C.M.A.; Silva, M.B.; Martins, P.F.A. Failure in single point incremental forming. Int. J. Adv. Manuf. Technol. 2015, 80, 1471–1479.
[4] Li, Y.; Daniel,W.J.T.; Meehan, P.A. Deformation analysis in single point incremental forming through finite element simulation. Int. J. Adv. Manuf. Technol. 2017, 88, 255–267.
[5] Ai, S.; Lu, B.; Chen, J.; Long, H.; Ou, H. Evaluation of deformation stability and fracture mechanism in incremental sheet forming. Int. J. Mech. Sci. 2017, 124–125, 174–184.
[6] Said, L.B.; Mars, J.; Wali, M.; Dammak, F. Numerical prediction of the ductile damage in single point incremental forming process. Int. J. Mech. Sci. 2017, 131–132, 546–558.
[7] Maqbool, F.; Bambach, M. Dominant deformation mechanisms in single point incremental forming (SPIF) and their effect on geometrical accuracy. Int. J. Mech. Sci. 2018, 136, 279–292.
[8] Esmaeilpour, R.; Kim, H.; Park, T.; Pourboghrat, F.; Mohammed, B. Comparison of 3D yield functions for finite element simulation of single point incremental forming (SPIF) of aluminum 7075. Int. J. Mech. Sci. 2017, 133, 544–554.
[9] Esmaeilpour, R.; Kim, H.; Park, T.; Pourboghrat, F.; Xu, Z.; Mohammed, B.; Farha, F.A. Calibration of Barlat Yld2004-18p yield function using CPFEM and 3D RVE for the simulation of single point incremental forming (SPIF) 7075-O aluminum sheet. Int. J. Mech. Sci. 2018, 145, 24–41.
[10] Mirnia, J.V.; Vahdani, M.; Shamsari, M. Ductile damage and deformation mechanics in multi-stage single point incremental forming. Int. J. Mech. Sci. 2018, 136, 396–412.
[11] Ilyas, M.; Hussain, G.; Espinosa, C. Failure and strain gradient analyses in incremental forming using GTN model. Int. J. Lightweight Mater. Manuf. 2019, 2, 177–185.
[12] Ai, S.; Long, H. A review on material fracture mechanism in incremental sheet forming. Int. J. Adv. Manuf. Technol. 2019, 104, 33–61.
[13] Shrivastava, P.; Tandon, P. Microstructure and texture based analysis of forming behavior and deformation mechanism of AA1050 sheet during single point incremental forming. J. Mater. Process. Technol. 2019, 266, 292–310.
[14] Mishra, S.; Yazar, K.U.; More, A.M.; Kumar, L.; Lingam, R.; Reddy, N.V.; Prakash, O.; Suwas, S. Elucidating the deformation modes in incremental sheet forming process: Insights from crystallographic texture, microstructure and mechanical properties. Mater. Sci. Eng. A 2020, 790, 139311.
[15] Hussain, G.; Ilyas, M.; Isidore, B.B.L.; Khan, W.A. Mechanical properties and microstructure evolution in incremental forming of AA5754 and AA6061 aluminum alloys. Trans. Nonf. Met. Soc. China 2020, 30, 51–64.
[16] Kumar, G.; Maji, K. Investigations into enhanced formability of AA5083 aluminum alloy sheet in single-point incremental forming. J. Mater. Eng. Perform. 2021, 30, 1289–1305.
[17] Lu, B.; Fang, Y.; Xu, D.K.; Chen, J.; Ai, S.; Long, H.; Ou, H.; Cao, J. Investigation of material deformation mechanism in double sided incremental sheet forming. Int. J. Mach. Tool. Manuf. 2015, 93, 37–48.
[18] Do, V.C.; Nguyen, D.T.; Cho, J.H.; Kim, Y.S. Incremental forming of 3D structured aluminum sheet. Int. J. Precis. Eng. Manuf. 2016, 17, 217–223.
[19] Do, V.C.; Pham, Q.T.; Kim, Y.S. Identification of forming limit curve at fracture in incremental sheet forming. Int. J. Adv. Manuf. Technol. 2017, 92, 4445–4455.
[20] Mirnia, M.J.; Shamsari, M. Numerical prediction of failure in single point incremental forming using a phenomenological ductile fracture criterion. J. Mater. Proc. Technol. 2017, 244, 17–43.
[21] Gatea, S.; Xu, D.; Ou, H.; McCartney, G. Evaluation of formability and fracture of pure titanium in incremental sheet forming. Int. J. Adv. Manuf. Technol. 2018, 95, 625–641.
[22] Yoganjaneyulu, G.; Narayanan, C.S.; Narayanasamy, R. Investigation on the fracture behavior of titanium Grade 2 sheets by using the single point incremental forming process. J. Manuf. Proc. 2018, 35, 197–204.

[23] Wang, H.; Wu, T.; Wang, J.; Li, J.; Jin, K. Experimental study on the incremental forming limit of the aluminum alloy AA2024 sheet. Int. J. Adv. Manuf. Technol. 2020, 108, 3507–3515.

[24] Zhan, X.;Wang, Z.; Li, M.; Hu, Q.; Chen, J. Investigations on failure-to-fracture mechanism and prediction of forming limit for aluminum alloy incremental forming process. J. Mater. Proc. Technol. 2020, 282, 116718.

[25] Yoganjaneyulu, G.; Raju, C.; Manikandan, N.; Narayanan, C.S. Investigations on multi-sheets single point incremental forming of commercial pure titanium alloys. Mater. Manuf. Proc. 2020, 35, 1002–1009.

[26] Kumar, G.; Maji, K. Formability of AA7075 sheet in single point incremental forming. Int. J. Manf. Mater. Mech. Eng. 2021, 11, 40–54.

[27] Jeswiet, J.; Adams, D.; Doolan, M.; McAnulty, T.; Gupta, P. Single point and asymmetric incremental forming. Adv. Manuf. 2015, 3, 253–262.

[28] Azevedo, N.G.; Farias, J.S.; Bastos, R.P.; Teixeira, P.; Davim, J.P.; de Sousa, R.J.A. Lubrication aspects during Single Point Incremental Forming for steel and aluminum materials. Int. J. Precis. Eng. Manuf. 2015, 16, 589–595.

[29] Behera, A.K.; Lu, B.; Ou, H. Characterization of shape and dimensional accuracy of incrementally formed titanium sheet parts with intermediate curvatures between two feature types. Int. J. Adv. Manuf. Technol. 2016, 83, 1099–1111.

[30] Lu, B.; Ou, H.; Shi, S.Q.; Long, H.; Chen, J. Titanium based cranial reconstruction using incremental sheet forming. Int. J. Mater. Form. 2016, 9, 361–370.

[31] Bastos, R.N.P.; Sousa, R.J.A.D.; Ferreira, J.A.F. Enhancing time efficiency on single point incremental forming processes. Int. J. Mater. Form. 2016, 9, 653–662.

[32] Vanhove, H.; Carette, Y.; Vancleef, S.; Duflou, J.R. Production of thin shell clavicle implants through Single Point Incremental Forming. Procedia Eng. 2017, 183, 174–179.

[33] Formisano, A.; Boccarusso, L.; Minutolo, F.C.; Carrino, L.; Durante, M.; Langella, A. Negative and positive incremental forming: Comparison by geometrical, experimental and FEM considerations. Mater. Manuf. Proc. 2017, 32, 530–536.

[34] Uheida, E.H.; Oosthuizen, G.A.; Dimitrov, D.M.; Bezuidenhout, M.B.; Hugo, P.A. Effects of the relative tool rotation direction on formability during the incremental forming of titanium sheets. Int. J. Adv. Manuf. Technol. 2018, 96, 3311–3319.

[35] Khan, S.; Hussain, G.; Ilyas, M.; Rashid, H.; Khan, M.I.; Khan, W.A. Appropriate heat treatment and incremental forming route to produce age hardened components of Al-2219 alloy with minimized form error and high formability. J. Mater. Process. Technol. 2018, 256, 262–273.

[36] Tera, M.; Breaz, R.E.; Racz, S.G.; Girjob, C.E. Processing strategies for single point incremental forming-a CAM approach. Int. J. Adv. Manuf. Technol. 2019, 102, 1761–1777.

[37] Palumbo, G.; Cusanno, A.; Romeu, M.L.G.; Bagudanch, I.; Negrini, N.C.; Villa, T.; Fare, S. Single Point Incremental Forming and Electrospinning to produce biodegradable magnesium (AZ31) biomedical prostheses coated with porous PCL. Mater. Today Proc. 2019, 7, 394–401.

[38] Kumar, A.; Gulati, V.; Kumar, P.; Singh, V.; Kumar, B.; Singh, H. Parametric effects on formability of AA2024-O aluminum alloy sheets in single point incremental forming. J. Mater. Res. Technol. 2019, 8, 1461–1469.

[39] Kumar, A.; Gulati, V. Experimental investigation and optimization of surface roughness in negative incremental forming. Measurement 2019, 131, 419–430.

[40] Oraon, M.; Sharma, V. Prediction of surface roughness in single point incremental forming of AA3003-O alloy using artificial neural network. Int. J. Mater. Eng. Innov. 2018, 9, 1–19.

[41] Su, C.; Zhao, Z.; Lv, Y.; Wang, R.; Wang, Q.; Wang, M. Effect of process parameters on plastic formability and microstructures of magnesium alloy in single point incremental forming. J. Mater. Eng. Perform. 2020, 28, 7737–7755.

[42] De Castro Maciel, D.; da Silva, G.C.; de Quadros, L.M. Incremental stamping forming with use of roller ball tool in aluminum and magnesium alloy. Int. J. Adv. Manuf. Technol. 2020, 108, 455–462.

[43] Maji, K.; Kumar, G. Inverse analysis and multiobjective optimization of single point incremental forming of AA5083 aluminum alloy sheet. Soft. Comput. 2020, 24, 4505–4521.

[44] Murugesan, M.; Jung, D.W. Formability and failure evaluation of AA3003-H18 sheets in single-point incremental forming process through the design of experiments. Materials 2021, 14, 808.

[45] Gatea, S.; Ou, H. Surface roughness analysis of medical grade titanium sheets formed by single point incremental forming. Int. J. Adv. Manuf. Technol. 2021, 1–16.

[46] Liu, Z. Heat assisted incremental sheet forming: A state-of-the-art-review. Int. J. Adv. Manuf. Technol. 2018, 98, 2987–3003.

[47] Ambrogio, G.; Gagliardi, F. Temperature variation in high speed incremental forming on different light weight alloys. Int. J. Adv. Manuf. Technol. 2015, 76, 1819–1825.

[48] Khazaali, H.; Saniee, F.F. A comprehensive experimental investigation on the influences of the process variables on warm incremental forming of Ti-6Al-4V alloy using a simple technique. Int. J. Adv. Manuf. Technol. 2016, 87, 2911–2923.

[49] Li, Z.; Lu, S.; Zhang, T.; Zhang, C.; Mao, Z. Electric assistance hot incremental sheet forming: An integral heating design. Int. J. Adv. Manuf. Technol. 2018, 96, 3209–3215.

[50] Bao,W.; Chu, X.; Lin, S.; Gao, J. Experimental investigation on formability and microstructure of AZ31B alloy in electropulseassisted incremental forming. Mater. Des. 2015, 87, 632–639.

[51] Husmann, T.; Magnus, C.S. Thermography in incremental forming processes at elevated temperatures. Measurement 2016, 77, 16–28.

[52] Gupta, P.; Jeswiet, J. Observations on heat generated in single point incremental forming. Procedia Eng. 2017, 183, 161–167.

[53] Gupta, P.; Jeswiet, J. Effect of temperatures during forming in single point incremental forming. Int. J. Adv. Manuf. Technol. 2018, 95, 3693–3706.

[54] Pacheco, P.A.P.; Silveira, M.E. Numerical simulation of electric hot incremental sheet forming of 1050 aluminum with and without preheating. Int. J. Adv. Manuf. Technol. 2018, 94, 3097–3108.

[55] Grimm, T.J.; Ragai, I. An investigation of liquid metal lubrication during electrically-assisted incremental forming of titanium. Procedia Manuf. 2019, 34, 118–124.

[56] Riaz, A.A.; Ullah, N.; Hussain, G.; Alkahtani, M.; Khan, M.N.; Khan, S. Experimental investigations on the effects of rotational speed on temperature and microstructure variations in incremental forming of T6-tempered and annealed AA2219 aerospace alloy. Metals 2020, 10, 809.

[57] Khazaali, H.; Saniee, F.F. Application of the Taguchi method for efficient studying of elevated-temperature incremental forming of a titanium alloy. J. Braz. Soc. Mech. Sci. Eng. 2018, 40, 1–9.

[58] Khazaali, H.; Saniee, F.F. Process parameters enhancement for incremental forming of a titanium Ti-6Al-4V truncated cone with varying wall angle at elevated temperatures. J. Braz. Soc. Mech. Sci. Eng. 2019, 20, 769–776.

[59] Leonhardt, A.; Kurz, G.; Victoria-Hernández, J.; Kräusel, V.; Landgrebe, D.; Letzig, D. Experimental study on incremental sheet forming of magnesium alloy AZ31 with hot air heating. Procedia Manuf. 2018, 15, 1192–1199.
[60] Liao, J.; Liu, J.; Zhang, L.; Xue, X. Influence of heating mode on orange peel patterns in warm incremental forming of magnesium alloy. Procedia Manuf. 2020, 50, 5–10.
[61] Mugendiran, V.; Gnanavelbabu, A. Comparison of plastic strains on AA5052 by single point incremental forming process using digital image processing. J. Mech. Sci. Technol. 2017, 31, 2943–2949.
[62] Lee, C.W.; Yang, D.Y. Study on the formability of magnesium alloy sheets in the incremental forming process with external heating sources. Int. J. Precis. Eng. Manuf. 2020, 21, 1519–1527.
[63] Singh, S.A.; Priyadarshi, S.; Tandon, P. Exploration of appropriate tool material and lubricant for elevated temperature incremental forming of aluminum alloy. Int. J. Precis. Eng. Manuf. 2021, 22, 217–225.